



25th ABCM International Congress of Mechanical Engineering
October 20-25, 2019, Uberlândia, MG, Brazil

GENERALIZED PROPORTIONAL DAMPING APPLIED TO A GUITAR MODEL

Alexandre M. Löw

Herbert M. Gomes

Universidade Federal do Rio Grande do Sul, Av. Sarmiento leite, 425, sala 202, 20. Andar, RS, Brazil
alexandre.low@ufrgs.br; herbert@mecanica.ufrgs.br

Gabriel S. Prado

Universidade Federal do Rio Grande do Sul, Av. Sarmiento leite, 425, RS, Brazil
gabriel_s_prado@hotmail.com

César M. A. Vasques

Departamento de Engenharia Mecânica, Universidade de Aveiro, Aveiro, Portugal
cmavasques@gmail.com

Abstract. *This work proposes an identification of damping considering the generalized-proportional (Rayleigh) damping approximation to a guitar finite element model. Estimates of the damping ratios (as well as natural frequencies) are experimentally obtained via random excitation in a free-free like condition and Subspace Stochastic Identification Covariance (SSI-Cov) analysis. First, the justification for the use of proportional damping approximation is verified by assuring that imaginary parts of selected modes are negligible when compared with their respective real parts. Then, a continuous function in the frequency domain is adjusted in such a way that it fits the identified damping ratios at their respective resonances. The curve fitting is obtained by non-linear least squares. Due to the size of the model, it would be impractical to manipulate full system matrices. Then, System Equivalent Reduction Expansion Process (SEREP) is applied to reduce the full model to the same number of measured degrees-of-freedom (DOF), still granting the same mode shapes as the full model. Thereafter, with the reduced system matrices, the same function fitted to the damping ratios is applied to the matrix product of the stiffness by the inverse mass in order to achieve the final goal that is to calculate the damping matrix. The practical appeal of the procedure can be evaluated when it is important to run a time-domain simulation of the structure and its transient response is to be compared with measured acceleration or displacement time histories.*

Keywords: *Generalized proportional damping, modal analysis, guitar vibroacoustics, SSI-Cov.*

1. INTRODUCTION

The complexity level of some structures, such as string instruments with acoustic chambers, makes it hard to obtain analytical solutions for the partial differential equations that govern their behavior, whether static, dynamic or modal, especially when considered the complete three-dimensional problem. Although there are simplified guitar models for modal analysis of low frequencies (Caldersmith et al. 1978; French, 2009), the importance of certain characteristics of structures, such as the reinforcements of the top plate, can only be evaluated with a three-dimensional model that contemplates, as well, this level of detail, which can be discretized for later numerical solution.

The finite element (FE) method currently occupies a prominent position among the computational tools to solve vibroacoustic problems. However, though computational methods have evolved tremendously since their appearance, in the mid-twentieth century, their application will always depend on a prior knowledge of the material and geometric features that define the structures, and about them there will always be some level of uncertainty, which will fatally be propagated on the model. As a consequence of this, the predicted results yielded by a FE model for the dynamic behavior of a structure generally differ to some degree from the experimental results, depending on the complexity of the structure and the level of uncertainty in the parameters supplied to the numerical model. For this reason, a great effort has been directed in the development of tools that correct FE models, either in the input parameters or directly in the mass and stiffness matrices (and possibly also damping), with data from an experimental modal analysis (Friswell and Mottershead, 1995; Maia et al. 1997). In this paper a generalized proportional damping matrix is calculated from the damping ratios extracted via SSI-Cov from simultaneously acquired acceleration histories of 8 points, 4 on the top and other 4 on the back plate (out of a total of 12 in the top and other 12 in the back), of a guitar resonant chamber. In

order to reduce the size of the system matrices, SEREP reduction is applied to the original 17,001 nodes FE model in such a way that calculations are performed accounting for approximately the same eight DOFs that were measured, even so maintaining the same analytic natural frequencies and the same mode shapes in these DOFs.

2. BRIEF LITERATURE SURVEY

2.1 Subspace Stochastic Identification

Subspace stochastic approach for experimental modal analysis can be classified as time-domain parametric, differing also from classic methods in that it naturally yields quantification of uncertainties in the identified parameters, as it considers randomness from its basic development rooted in control theory state-space formulation. The foundations of this method were laid by classic textbooks, e.g., van Overschee and de Moor (1996), but it continues to experiment great improvements and application, especially in modal analysis of large-sized civil structures.

Two major variants of SSI theory are strongly established: data-driven (SSI-Data) and covariance-driven (SSI-Cov). In Rainieri and Fabbrocino (2011), SSI theory is presented with focus on these two approaches, among other methods for operational modal analyses. A real structure example is presented too, so that some assessment can be made for the suitability of the method. Beyond this, among other important aspects, it is showed also a way to circumvent the lack of mass-normalization in the identified modes, present in every operational (output-only) procedure, by measuring the structure a second time with well-defined lumped mass changes.

2.2 System Equivalent Reduction Expansion Process (SEREP)

Analysis of large complex structures by discretization-based computational methods, such as the finite element method (FEM) and boundary element method (BEM), gave rise to the need of lower order equivalent models still capable of represent the most important dynamical features of their full-sized counterparts. Friswell and Mottershead (1995) have presented classic reduction algorithms such as static (Guyan) and dynamic condensation, where partitions are made in the system matrices (mass and stiffness). The ability of the models created by these procedures to correctly predict modal parameters depends strongly on the choice of retained degrees of freedom (DOFs). This motivated improvements, and more recently other methods have been chosen. In Marwala (2010), the theory of static and dynamic condensation is presented along with Improved Guyan and System Equivalent Reduction Expansion Process (SEREP) as the best practices for model order reduction.

2.3 Generalized Proportional Damping

The idea of a generalized proportional damping finds its roots on the classic work of Lord Rayleigh (1877), in the beginnings of what is now known as the theories of mechanical vibrations and sound generation. This simplified model had the great advantage of producing only normal modes (with null imaginary parts), and that such a damping matrix is diagonalizable by the same modal matrix as the undamped system.

Later, Caughey and O'Kelly (1965) have written the necessary conditions for a viscously damped system to possess classical normal modes and explored much further the forms of the damping matrix that still produce only real-valued mode shapes.

Broadening still further these conditions, Adhikari and Woodhouse (2000) proposed a method for identification of the damping matrix based on a curve fitting of identified frequencies vs. damping ratios, then applied the fitted function to the product of the inverse mass matrix by the stiffness matrix.

3. COVARIANCE DRIVEN STOCHASTIC SUBSPACE IDENTIFICATION SSI-COV

In many applications, the dynamic behavior of a mechanical system can be conveniently defined by a state space model. Such a formulation is used to convert a system of second order differential equations into a set of two systems of first order differential equations defined by the so-called state equation and the observation equation. For a simple second order differential equation of motion of the type

$$\mathbf{M} \ddot{\mathbf{y}}(t) + \mathbf{D} \dot{\mathbf{y}}(t) + \mathbf{K} \mathbf{y}(t) = \mathbf{B} \mathbf{u}(t) = \mathbf{F}(t) \quad (1)$$

where \mathbf{M} , \mathbf{D} and \mathbf{K} are the mass, damping and stiffness matrices and \mathbf{B} is the incidence matrix for the input vector $\mathbf{u}(t)$. Assuming a variable transformation where $\mathbf{q}(t) = [\ddot{\mathbf{y}}(t) \ \dot{\mathbf{y}}(t)]^T$, the corresponding state space model is defined as

$$\begin{aligned} \dot{\mathbf{q}}(t) &= \mathbf{A}_c \mathbf{q}(t) + \mathbf{B}_c \mathbf{u}(t) \\ \mathbf{q}(t) &= \mathbf{C}_c \mathbf{q}(t) + \mathbf{D}_c \mathbf{u}(t) \end{aligned} \quad (2)$$

where, $\mathbf{C}_c = [\mathbf{C}_v - \mathbf{C}_a \mathbf{M}^{-1} \mathbf{D} \quad \mathbf{C}_d - \mathbf{C}_a \mathbf{M}^{-1} \mathbf{K}]$ is the output influence matrix, with \mathbf{C}_v and \mathbf{C}_d being the observations matrices for velocities and displacements, $\mathbf{D}_c = \mathbf{C}_a \mathbf{M}^{-1} \mathbf{B}$ is the direct transmission matrix, \mathbf{C}_a being the observation matrix for measured acceleration, and

$$\mathbf{A}_c = \begin{bmatrix} -\mathbf{M}^{-1} \mathbf{D} & -\mathbf{M}^{-1} \mathbf{K} \\ \mathbf{I} & \mathbf{0} \end{bmatrix}, \quad \mathbf{B}_c = \begin{bmatrix} -\mathbf{M}^{-1} \mathbf{B} \\ \mathbf{0} \end{bmatrix}. \quad (3)$$

The idea behind the Stochastic Subspace Identification methods is to measure a large amount of outputs $\mathbf{y}(t)$ in order to identify \mathbf{A}_c and \mathbf{C}_c . An assumed stochastic uncorrelated process white noise \mathbf{w} and measurement noise \mathbf{v} will exist in the real system in equation (2), so one can assure that the system response in the state space model is represented by a zero mean Gaussian process and the output covariance matrix $\mathbf{R} = E[\mathbf{y}(t + \Delta t) \mathbf{y}(t)^T]$, where $E[\cdot]$ is the expected value operator, and the state space vector $\boldsymbol{\Sigma} = E[\mathbf{q}(t + \Delta t) \mathbf{q}(t)^T]$. Thus, the expected value of the convolution $E[\mathbf{q}(t) \mathbf{w}(t)^T] = \mathbf{0}$ and $E[\mathbf{q}(t) \mathbf{v}(t)^T] = \mathbf{0}$ (Van Overschee and de Moor, 1996). After some algebraic manipulations, one finds

$$\boldsymbol{\Sigma} = \mathbf{A} \boldsymbol{\Sigma} \mathbf{A}^T + \mathbf{Q}^{ww} \text{ and } \mathbf{G} = E[\mathbf{q}(t) \mathbf{y}(t)^T] = \mathbf{A} \boldsymbol{\Sigma} \mathbf{C}^T + \mathbf{S}^{ww}. \quad (4)$$

Then, starting from the data matrix $\mathbf{Y}_{l \times N}$ (l means the number of measured channels and N the number of repetitions of measurements), one calculates the unbiased estimate of the correlation matrix (Zhang *et al.*, 2005) at time i , $\mathbf{R}_i = \mathbf{Y}_{1, \dots, N-i} \mathbf{Y}_{i, \dots, N}^T$. Thus, for different time lags, one can assemble the Toeplitz matrix

$$\mathbf{T}_{1|i} = \begin{bmatrix} \mathbf{R}_i & \cdots & \mathbf{R}_{i-1} \cdots \mathbf{R}_1 \\ \vdots & & \ddots & \vdots \\ \mathbf{R}_{2i-1} & \cdots & \mathbf{R}_{2i-2} \cdots \mathbf{R}_i \end{bmatrix}. \quad (5)$$

By singular value decomposition (SVD) of the Toeplitz matrix, one finds $\mathbf{T}_{1|i} = \mathbf{U}_1 \boldsymbol{\Sigma}_1 \mathbf{V}_1^T$. The identified state space matrix \mathbf{A} is obtained by $\mathbf{A} = \boldsymbol{\Sigma}_1^{-1/2} \mathbf{U}_1^T \mathbf{T}_{2|i} \mathbf{V}_1 \boldsymbol{\Sigma}_1^{-1/2}$ and the modal parameters are obtained by $\mathbf{A} = \boldsymbol{\Psi} \mathbf{M} \boldsymbol{\Psi}^{-1}$, $\boldsymbol{\Phi} = \mathbf{C} \boldsymbol{\Psi}$. The eigenvalues converted into continuous time are obtained by the diagonal terms of the matrix \mathbf{M} as $\lambda_m = \ln(\mu_m) / \Delta t$, and the corresponding undamped natural frequencies and damped natural frequencies obtained by $\omega_{n,r} = |\lambda_{m,r}|$ and $\omega_{d,r} = \text{Im}(\lambda_{m,r})$, and the damping ratio obtained by $\zeta_r = -\text{Re}(\lambda_{m,r}) / |\lambda_{m,r}|$. The stabilization diagram (order of the system versus identified parameter) is used to determine the adequate system order n to be used in the identification by the stabilization of natural frequencies and damping ratio poles between increasing orders (Rainieri and Fabbrocino, 2011).

4. SYSTEM EQUIVALENT REDUCTION EXPANSION PROCESS (SEREP)

In order to reduce the size of the mechanical model the System Equivalent Reduction Expansion Process (SEREP) was chosen because this method a priori imposes that eigenproperties of the reduced system always equals those of the full system for the modes of interest (retained in the reduced model). Also, the modes that are preserved in the reduced model may be arbitrarily selected from those modes of interest in the original model and, more importantly, the eigensolution of the reduced system is *exact* regardless of the location or number of points preserved in the reduced model (Marwala, 2010). Another interesting feature is that one can arbitrarily select the included DOFs in the reduced model so that their locations reproduce the set of measured points. Then, starting from separation of \mathbf{x}_a active and \mathbf{x}_d deleted from the complete set of DOFs (\mathbf{x}_n), and assuming separability between mode shapes and time varying modal coordinates $\mathbf{q}(t)$,

$$\mathbf{x}_n(t) = \begin{bmatrix} \mathbf{x}_a(t) \\ \mathbf{x}_d(t) \end{bmatrix} = \boldsymbol{\Phi}_n \mathbf{q}(t) = \begin{bmatrix} \boldsymbol{\Phi}_a \\ \boldsymbol{\Phi}_d \end{bmatrix} \mathbf{q}(t) \quad \text{and} \quad \mathbf{x}_a(t) = \boldsymbol{\Phi}_a \mathbf{q}(t). \quad (6)$$

In a least square sense, one can find that

$$\mathbf{q}(t) = [\boldsymbol{\Phi}_a^T \boldsymbol{\Phi}_a]^{-1} \boldsymbol{\Phi}_a^T \mathbf{x}_a(t) = \boldsymbol{\Phi}_a^+ \mathbf{x}_a, \quad (7)$$

where the $^+$ sign means the pseudo-inverse of vector $\boldsymbol{\Phi}_a$. Substituting this into the modal transformation, yields

$$\begin{bmatrix} \mathbf{x}_a \\ \mathbf{x}_d \end{bmatrix} = \begin{bmatrix} \boldsymbol{\Phi}_a \\ \boldsymbol{\Phi}_d \end{bmatrix} \boldsymbol{\Phi}_a^+ \mathbf{x}_a. \quad (8)$$

Therefore, the SEREP transformation matrix can now be written as

$$\mathbf{T}_u = \boldsymbol{\Phi}_n \boldsymbol{\Phi}_a^+ = \begin{bmatrix} \boldsymbol{\Phi}_a [\boldsymbol{\Phi}_a^T \boldsymbol{\Phi}_a]^{-1} \boldsymbol{\Phi}_a^T \\ \boldsymbol{\Phi}_d [\boldsymbol{\Phi}_d^T \boldsymbol{\Phi}_d]^{-1} \boldsymbol{\Phi}_d^T \end{bmatrix}. \quad (9)$$

The reduced mass and stiffness matrices, $\mathbf{M}_a^{\text{red}}$ and $\mathbf{K}_a^{\text{red}}$, can finally be evaluated as

$$\mathbf{M}_a^{\text{red}} = \mathbf{T}_u^S \mathbf{M}_n \mathbf{T}_u = \boldsymbol{\Phi}_a^{+T} \boldsymbol{\Phi}_a^+ \quad \text{and} \quad \mathbf{K}_a^{\text{red}} = \mathbf{T}_u^S \mathbf{K}_n \mathbf{T}_u = \boldsymbol{\Phi}_a^{+T} \boldsymbol{\Omega}^2 \boldsymbol{\Phi}_a^+. \quad (10)$$

If they are used in the corresponding eigenvalue eigenvector problem, this will result in a reduced number of frequencies and mode shapes that exactly match the frequencies and mode shapes of the original system for the selected active DOFs.

5. GUITAR MODEL

The 3D FE model of a guitar was built using Ansys Parametric Design Language (APDL) and the proper geometric parameters were measured and estimated based on laboratory tests performed previously. The FE model is composed of 8-node Ansys shell-281 elements, with 3 translations and 3 rotations per node. A convergence test for eigenvalues was performed and a characteristic mesh size of 3.75 mm was found as appropriate for this problem. The generated FE model has 17001 nodes with 102,006 DOFs. The boundary conditions were set according to the experimental setup as a free-free boundary condition in order to minimize the effects of uncertainty in the constraints. The composite wood plates for upper and lower sound board were defined based on manufacturer indications as well as the material properties for the type of wood and fiber orientation for layup. The internal bracing is of classic 5 bar fan type.

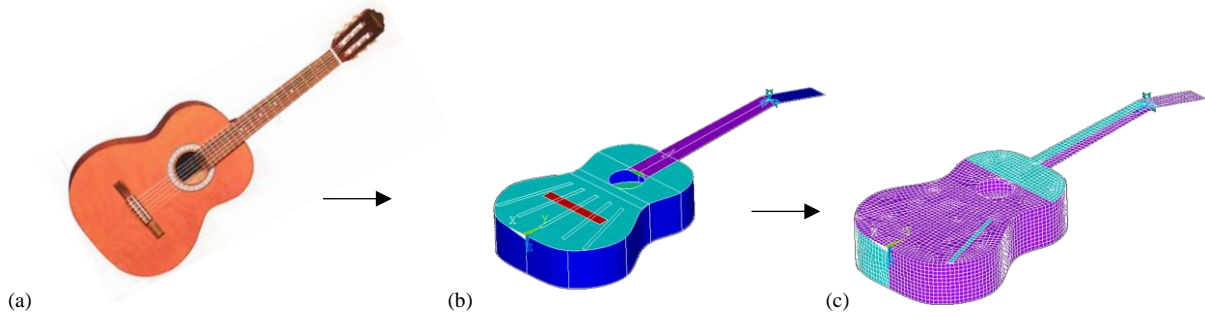


Figure 1. (a) Actual guitar model, (b) material definition and (c) the corresponding FE mesh.

The main mode shapes, using the nominal values for the guitar, apart from the three initial rigid body modes, are presented in Figure 2.

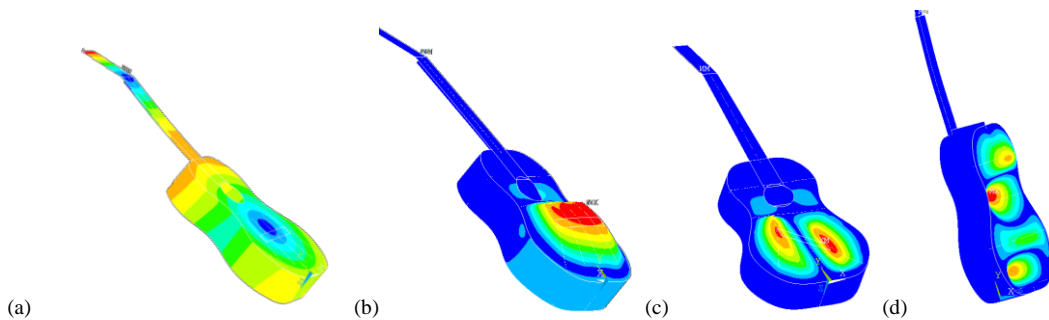


Figure 2. Main mode shapes for the guitar in the free-free boundary condition (rigid body modes omitted): (a) torsion of the arm and bending of upper-soundboard (75.9 Hz), (b) 1st bending of the bottom half of upper-soundboard (110.2 Hz), (c) out of phase 2nd bending of the bottom half of upper soundboard (169.3 Hz) and (d) out of phase 3rd bending of the lower soundboard (174.1Hz).

In the experimental setup, the locations of the accelerometers were determined by visual inspection of mode shapes calculated with the FE model in such a way that all of them are sufficiently excited by the chosen modes. The exact positions were measured and a plain text file was written with this information to be read during the FE simulation (after the solution phase) to find the closest nodes, and corresponding DOFs, and so extract the modal matrix just for these DOFs (active) and chosen modes. These positions are listed in the table below.

Table 1: Locations of the measured points [mm].

	X	Y	Z
1	0	54	0
2	-65	220	0
3	50	324	0
4	-65	410	0
5	0	147	105
6	-65	220	105
7	50	324	105
8	-65	410	105

The coordinate system was positioned in the bottom edge of the top plate over its line of symmetry, with Z axis pointing to the back plate, X axis pointing to the right (looking to the varnished side of the top plate) and Y axis pointing upwards (to the nut).

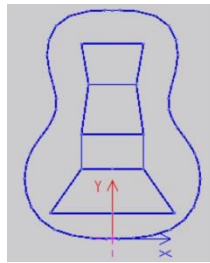


Figure 3. Axes positions and orientations, and grid of measured locations

For comparison with measured results, the direct inertance frequency response function (FRF) at the bridge, and a cross inertance FRF between the bridge and a point in the middle of the back plate, are presented below in Figure 3. These FRFs were acquired with an instrumented hammer and a micro accelerometer Endevco A110.

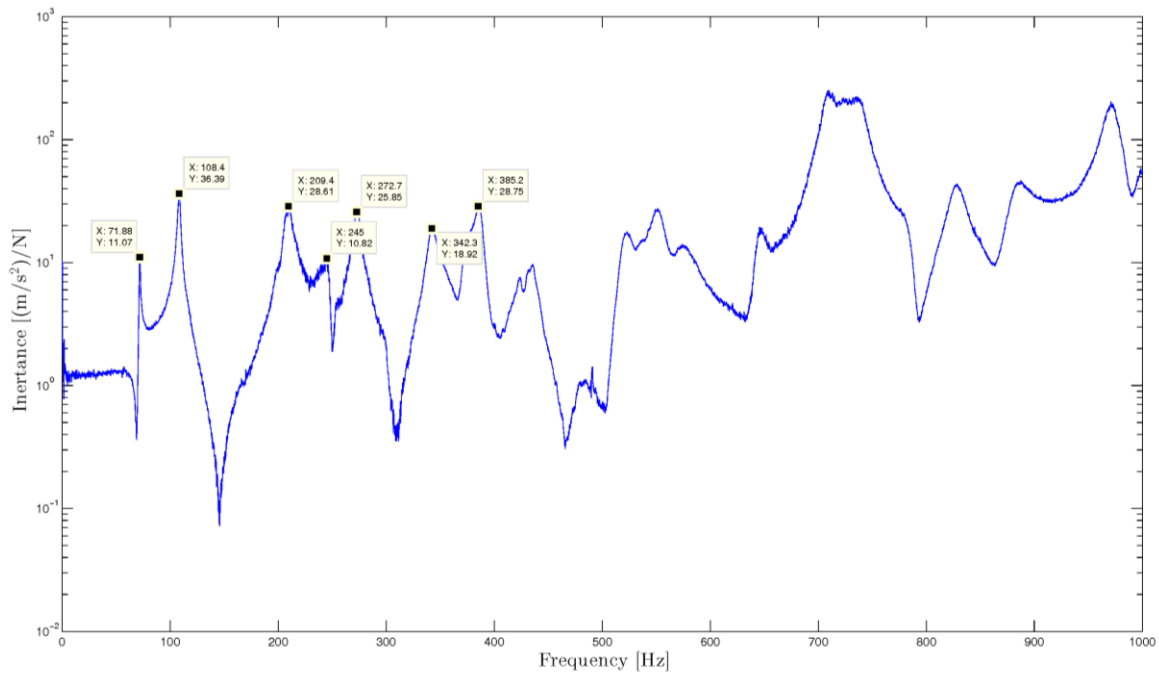


Figure 4. Typical inertance FRF excited by impact hammer at the bridge and measured at the back plate.

6. GENERALIZED PROPORTIONAL DAMPING

The idea of a proportional damping (mass and stiffness) has been used for a long time for several problems, but this approach seems not suitable since arbitrary variation of damping ratio with respect to vibration frequency is not possible. Once defined the proportionality factors of damping based on mass and stiffness, the ratio for the damping at several vibration frequency become fixed. Adhikari (2006) presented a generalized proportional damping model to overcome this problem that is based in measuring the damping for each vibration frequency and then fitting a polynomial function that passes throughout all the points. Afterwards, a power series of the type $\mathbf{C} = \mathbf{M} \sum_{j=0}^{n-1} \alpha_j (\mathbf{M}^{-1} \mathbf{K})^j$ assures the necessary and sufficient condition for the existence of classical normal modes. Thus, proportional viscously damped linear systems will have normal mode shapes $\Phi^T \mathbf{C} \Phi = 2\zeta \Omega = \beta_1(\Omega^2) + \Omega^2 \beta_2(\Omega^{-2})$, where $\beta_i(\cdot)$ are smooth analytic functions in the neighborhood of all the eigenvalues of their arguments.

Then, in order to identify a proportional damping matrix, natural frequencies and damping ratios were obtained with SSI-Cov procedure. Below is the stabilization chart plotted with the auto power spectral density of the 1st channel, where it can be seen that a robust stabilization was achieved already at relatively low order modes. After careful assessment of the results, it was determined that order 54 resulted in 19 stabilized modes for frequency and damping, with these resonances having precise correspondence with the peaks observed in the graphic.

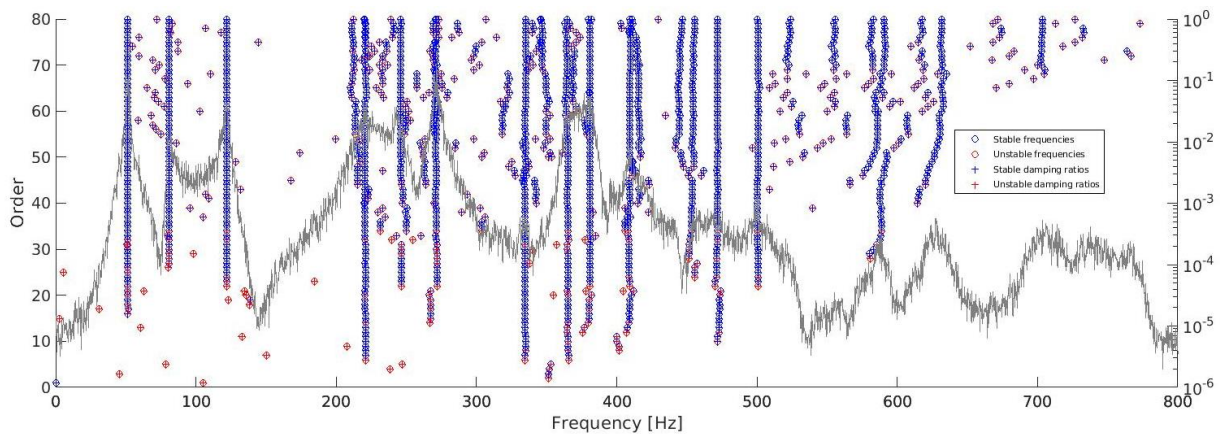


Figure 5. Stabilization diagram for the identified frequencies and damping against A-PSD.

Then, with the set of modal parameters calculated in the previous step, a seventh degree polynomial curve fitting was applied to the damping ratios vs. natural frequencies pairs yielded by SSI-Cov. The fitted curve is showed in the following figure.

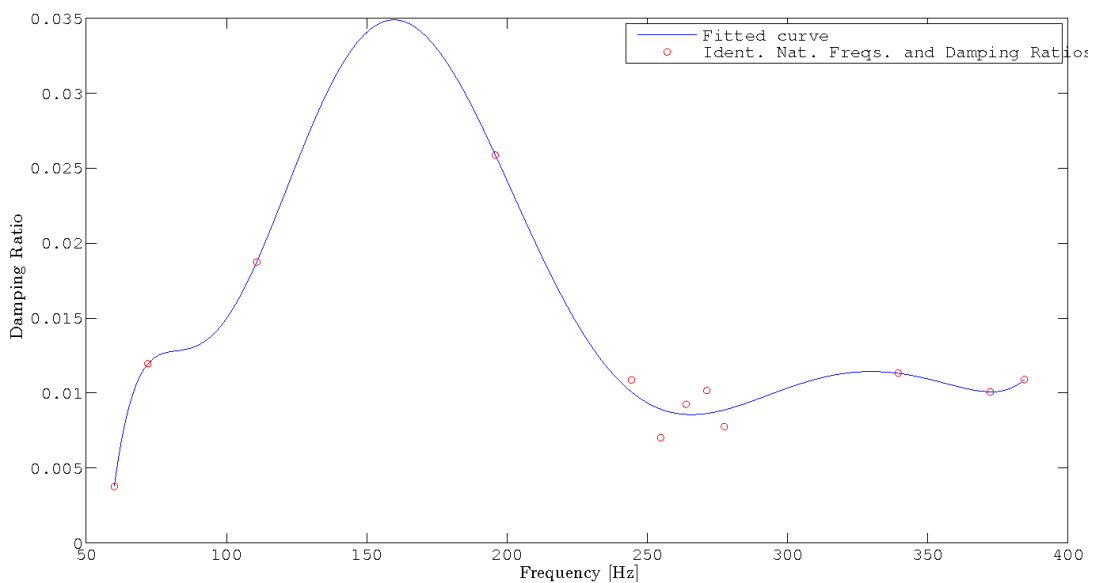


Figure 6. Curve fitting of 7th degree polynomial to the 12 identified natural frequencies vs. damping ratio points.

Finally, applying the same seventh degree polynomial to the matrix ($\mathbf{\Omega}^2 = \mathbf{M}^{-1}\mathbf{K}$), and treating products (powers) with matrix (non-commutative) algebra, the proportional damping matrix is calculated according to the equation presented above. To compare this result, the inertance (acceleration divided by force) FRF was generated with reduced model matrices and plotted against previously measured FRFs by impact testing in the same points.

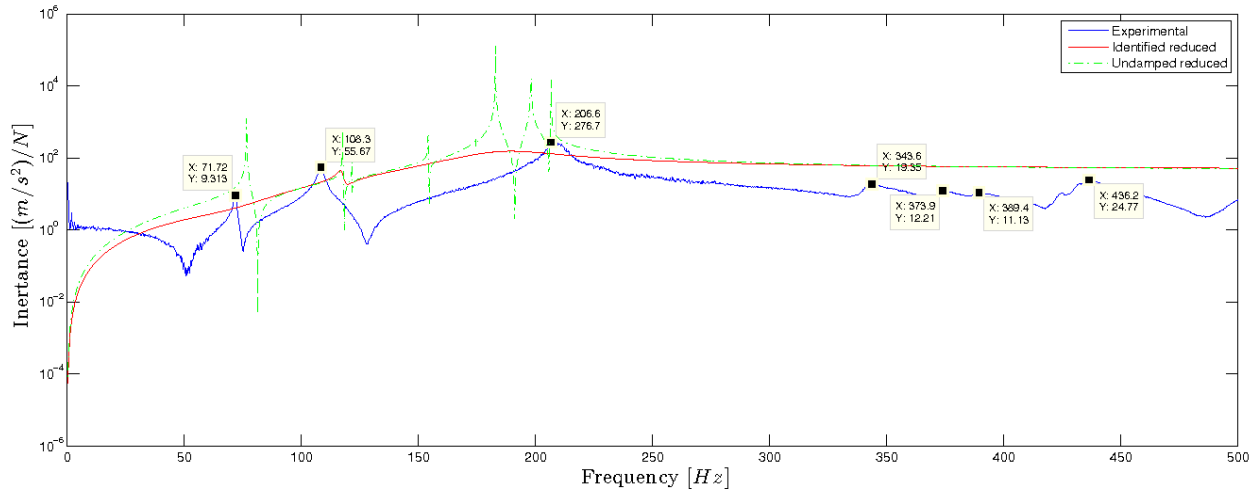


Figure 7. Experimental vs. reduced (computational) inertances.

7. CONCLUSIONS

A generalized proportional damping matrix was identified for a large FE model of a classic acoustic guitar. The size of system matrices makes it unfeasible to perform some calculations using the whole set of model DOFs, so model reduction was successfully applied to the original model, retaining the numerical DOFs that were closest to the chosen eight measured ones. So the first eight natural frequencies and damping ratios were taken from a set of nineteen sets of modal parameters identified with SSI-Cov technique. Stabilization diagram revealed that a robust identification in the selected frequency range was achieved.

Curve fitting was done with the vector of damping ratios vs. the vector of natural frequencies, and a polynomial was uniquely fitted to the data in order to determine its coefficients.

SEREP condensation was applied to reduce the order of the model and the resulting small size matrices can still yield exactly the same modal parameters as the undamped original system, in the frequency range of interest, for the retained set of DOFs. With the reduced matrices, the calculations inside the fitted polynomial with matrix argument were made possible, and so a fully populated damping matrix was obtained.

The analytical inertance FRFs (calculated with the reduced matrices) were traced against experimental ones, and revealed that there are still significant deviations. These differences might be primarily a result of inconsistencies in the computational model, and in this case a model updating procedure should greatly improve the results. Even so, some agreement for frequency, amplitude and damping level for at least one major peak suggests that the overall procedure is promising.

8. REFERENCES

- Adhikari, S., 2006. Damping modelling using generalized proportional damping. *Journal of Sound and Vibration*, 293(1–2):156-170.
- Adhikari, S.; Woodhouse, J., 2001. Identification of damping: part 1: Viscous damping. *Journal of Sound and Vibration*, 243(1):43-61.
- Ansys, 2018. *Academic Research Mechanical*, Release 18.0.
- Caldersmith, G., 1978. Guitar as a Reflex Enclosure, *Journal of the Acoustical Society of America*, 63(5):1566-1575.
- Caughey, T. K., O'Kelly, M. E. J., 1965. Classical normal modes in damped linear dynamic systems. *ASME Journal of Applied Mechanics*, 32:583–588.
- French, M., 2009. *Engineering the Guitar: Theory and Practice*. Springer Verlag, New York.
- Friswell, M. I. and Mottershead, J. E., 1995. *Finite Element Model Updating in Structural Dynamics*. Kluwer Academic Publishers, Dordrecht.
- Maia, N. M. M., Silva, J. M. M. et al., 1997. *Theoretical and Experimental Modal Analysis*. Editors: Maia, N. M. M and Silva, J. M. M. Research Studies Press, England.

- Marwala, T., 2010. *Finite-element-model Updating Using Computational Intelligence Techniques - Applications to Structural Dynamics*. Springer-Verlag, London.
- Matlab, 2012. *MATrix LABoratory, R2012a*. The MathWorks Inc., Natick, MA.
- Rainieri C., Fabbrocino G., 2014. *Operational Modal Analysis of Civil Engineering Structures: An Introduction and Guide for Applications*. Springer-Verlag, London.
- Rainieri C., Fabbrocino G., 2011. Performance assessment of selected OMA techniques for dynamic identification of geometrical systems and closely spaced structural modes, *Journal of Theoretical and Applied Mechanics*, 49: 825-839.
- Rayleigh, J. W., 1877. *Theory of Sound* (2 volumes), 2nd edition, Dover Publications, New York, 1945 re-issue.
- Shanke, S. A., 2015. *Operational Modal Analysis of Large Bridges*. NTNU Doctoral Thesis. Trondheim.
- Van Overschee, P., de Moor, B., 1996. *Subspace Identification for Linear Systems*. Kluwer Academic Publisher, Boston.
- Zhang, Y., Zhang, Z., Xu, X. and Hua, H., 2005. Modal Parameter Identification Using Response Data Only, *Journal of Sound and Vibration*, 282(1-2): 367-380.

9. RESPONSIBILITY NOTICE

The authors are the only ones responsible for the printed material included in this paper.